Dielectric Relaxation Studies on Molecular Motion of Poly(fluoroalkyl α-substituted acrylate)s and Compass Motion Model for Internal Motion of the Fluoroalkyl Side Chain

Kenji Tadano,*,† Yoshito Tanaka,‡ Tetsuo Shimizu,‡ and Shinichi Yano*,§

Gifu College of Medical Technology, Ichihiraga, Seki, Gifu 501-3892, Japan; R & D Department, Daikin Industries Ltd., Settsu, Osaka 566-8585, Japan; and Department of Chemistry, Faculty of Engineering, Gifu University, Yanagido, Gifu 501-1193, Japan

Received July 2, 1998; Revised Manuscript Received December 9, 1998

ABSTRACT: Dielectric measurements were made on poly(fluoroalkyl α-substituted acrylate)s, $-[-CH_2-CX(COO(CH_2)_m(CF_2)_nY)-]_p-$ [PX−Hm−Fn−Y, X = α-substituent (F, Cl, Me, H), Y = F or H], over a wide temperature range from 90 to 530 K at different frequencies between 100 Hz and 100 kHz. In the PF−Hm−Fn−Y polymers, there were observed three relaxations, α above 400 K, β around 250 K, and γ below 150 K, which were attributed to a reorientational motion of long segments above T_g, a rotational motion of carbonyl groups in amorphous region, and an internal motion of fluoroalkyl side chains, respectively, based on the assignments of poly(*n*-alkyl methacrylate)s. As the fluoroalkyl length ($N_c = m + n$) increases, the γ relaxation shifted to higher temperatures in PF−Hm−Fn−F but was almost unchanged in PF−Hm−Fn−H, while the α relaxation moved to higher temperatures in both polymers. This dielectric relaxation behavior was well explained by the chemical structures and the existence of crystallites (the ordering of main backbone chains and fluoroalkyl chains). It is noted that the activation enthalpy for the γ relaxation [$\Delta H(\gamma)$] increases with increasing N_c. The $\Delta H(\gamma)$ values for PF−H1−Fn−F were well consistent with the vaporization enthalpy (ΔH_{vap}) of the corresponding C_nF_{2n+2}, but those for PF−H1−Fn−H were larger than for PF−H1−Fn−F. These characteristic changes of $\Delta H(\gamma)$ with N_c were well explained by compass motion model newly proposed in this paper, in which the fluoroalkyl side chain moves on an orbit drawn by a compass to make the γ relaxation: It was found that $\Delta H(\gamma)$ for PF−H1−Fn−F is almost consistent with ΔH_{vap} (the sum of the energy in intramolecular interaction (ΔH_{intra}) and intermolecular interaction (ΔH_{inter})), while the larger $\Delta H(\gamma)$ value for PF−H1−Fn−H is related to the existence of H- - -F hydrogen bonding of the terminal $-CF_2-H$ with F whose energy (ΔH_{coul}) was calculated by assuming Coulomb attraction.

Introduction

Recently, scientific interest has been increasing for a class of poly(fluoroalkyl α-substituted acrylate)s (denoted as PX−Hm−Fn−Y in Figure 1) which are a comb-shaped polymers having the fluoroalkyl esters as the side chains, because the fluoroalkyl side chains frequently generate unique structures and properties due to the ordering of the side chains.[1−13]

Poly(fluoroalkyl acrylate)s (PX−Hm−Fn−Y) and poly(fluoroalkyl methacrylate)s (PX−Hm−Fn−Y) have been found to be crystalline, when the length of the fluoroalkyl side chains ($N_c = m + n$) is larger than 7;[8,9] the fluoroalkyl side chains are packed into a double-layer structure in PX−Hm−Fn−Y and both double- and single-layer structures in PX−Hm−Fn−Y to form the crystallites, while when $N_c \leq 7$, both polymers are amorphous. When temperature increases, the double-layer packings in PX−Hm−Fn−Y, which coexist with the single-layer packings, transformed into the single-layer packings between 366 and 389 K.

In preceding papers,[10−12] we reported the ordered structures and properties of a series of poly(fluoroalkyl α-fluoroacrylate)s (PF−Hm−Fn−Y). We found that the PF−Hm−Fn−Y polymers are crystalline even in the shorter fluoroalkyl homologues with $N_c < 7$, for example even in PF−H1−F1−F, and noticeably, the crystallites

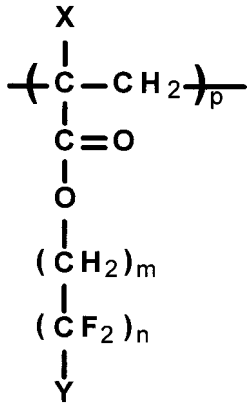

Figure 1. Chemical structures of poly(fluoroalkyl α-substituted acrylate)s (PX−Hm−Fn−Y). X = α-substitutent, H, M(CH_3), F, C(Cl); Y = H or F; *m* = number of CH_2; *n* = number of CF_2; $N_c = n + m$ = fluoroalkyl length.

are formed by the orderings of not only the side chains but also the main backbone chains. In the shorter fluoroalkyl homologues with $N_c < 7$, the ordering of main backbone chains is predominant, and the side chains are arranged in double-layer packings at room temperature. With increasing temperature, the double-layer packings are more ordered above T_g due to the disturbing (softening) of the ordered main backbone chains and then begin to be more gradually disturbed with increasing temperature. In the longer fluoroalkyl homologues with $N_c > 7$, on the other hand, the ordering of the side chains predominates in the formation of

† Gifu College of Medical Technology.
‡ Daikin Industries, Ltd.
§ Gifu University.

10.1021/ma981048o CCC: $18.00
Published on Web 02/12/1999

Table 1. List of Polymers Used Here

polymer	α-substituent	alkyl group	MW ($\times 10^5$)	$[\eta]$ (dL g^{-1})[a]	triad stereoregularity mm	mr	rr	T_g (K)	T_m (K)	ΔH_m (kJ mol^{-1})
PF−H1−F1−F	F	$-CH_2-CF_2-F$	2.6	0.68	0.13	0.50	0.37	383	487	1.3
PF−H1−F2−F	F	$-CH_2-(CF_2)_2-F$	1.8	0.53	0.12	0.48	0.40	370	493	3.5
PF−H1−F3−F	F	$-CH_2-(CF_2)_3-F$		0.19	0.11	0.49	0.40	348	460	4.0
PF−H1−F4−F	F	$-CH_2-(CF_2)_4-F$			0.12	0.46	0.42	336	444	3.4
PF−H1−F7−F	F	$-CH_2-(CF_2)_7-F$			0.10	0.49	0.41		454	4.8
PF−H1−F8−F	F	$-CH_2-(CF_2)_8-F$			0.13	0.46	0.41		458	5.3
PF−H1−F9−F	F	$-CH_2-(CF_2)_9-F$			0.12	0.45	0.43		469	6.0
PF−H1−F11−F	F	$-CH_2-(CF_2)_{11}-F$			0.11	0.47	0.42		472	7.7
PF−H1−F2−H	F	$-CH_2-(CF_2)_2-H$	2.2	0.53	0.12	0.47	0.41	359	449	0.4
PF−H1−F4−H	F	$-CH_2-(CF_2)_4-H$	7.0	0.99	0.11	0.48	0.41	328	414	1.6
PF−H1−F6−H	F	$-CH_2-(CF_2)_6-H$	4.4	0.57	0.13	0.46	0.41		416	2.6
PF−H1−F8−H	F	$-CH_2-(CF_2)_8-H$	3.7	0.27	0.11	0.56	0.33		432	4.8
PF−H2−F4−F	F	$-(CH_2)_2-(CF_2)_4-F$		0.41[b]	0.12	0.49	0.39	279	364	0.4
PF−H2−F6−F	F	$-(CH_2)_2-(CF_2)_6-F$		0.27[b]	0.14	0.49	0.37	326	377	0.7
PF−H2−F8−F	F	$-(CH_2)_2-(CF_2)_8-F$		0.24[b]	0.16	0.50	0.34	333[c]	399	1.9
PF−H2−F10−F	F	$-(CH_2)_2-(CF_2)_{10}-F$			0.13	0.49	0.38	326	430	9.4
PH−H2−F8−F	H	$-(CH_2)_2-(CF_2)_8-F$		0.37[b]	0.06	0.51	0.43	325	349	8.4
PM−H2−F8−F	CH_3	$-(CH_2)_2-(CF_2)_8-F$		0.37[b]	0.05	0.45	0.50	330	361	3.7
PC−H2−F8−F	Cl	$-(CH_2)_2-(CF_2)_8-F$		0.15[b]	0.05	0.73	0.22	334	404	5.1
PF−HFIP	F	$-CH-(CF_3)_2$	3.1		0.09	0.47	0.44	375		
PF−H2−H	F	$-(CH_2)_2-H$	1.8		0.14	0.50	0.36	367		
PF−H3−H	F	$-(CH_2)_3-H$	1.9		0.14	0.48	0.38	335		

[a] Data in ethyl acetate. [b] Data in 1,3-bis(trifluoromethyl)benzene. [c] Quenched sample.

crystallites but is somewhat perturbed by the weakly ordered main backbone chains. As a result, the side chains are packed into the single-layer packings which transformed into the double-layer packings around T_g with increasing temperature. Consequently, the PF−Hm−Fn−Y polymers have the ordered structure formed by both fluoroalkyl side and main backbone chains, and this ordering is also found in the PC−Hm−Fn−Y polymers. However, the PX−Hm−Fn−Y and PX−Hm−Fn−Y polymers have the crystallites only when $N_c > 7$ which are formed only by the ordering of the fluoroalkyl side chains.

Some of PX−Hm−Fn−Y polymers are known to have low refractive index, good optical transparency, and low surface energy and hence have been used as clad materials for optical fibers and oil- and water-repellent agents and moisture-proof coatings.[5−7,14,15] These outstanding properties should be modified by both crystallites and segmental molecular motion which are temperature-dependent.

Previously, we reported the preliminary dielectric relaxation studies of several PF−Hm−Fn−Y and PX−Hm−Fn−Y homologues.[13] Both polymers had α and γ relaxations which are attributed to a reorientational molecular motion of long segments above T_g and a local molecular motion of the fluoroalkyl side chains below T_g, respectively, being analogous to those for poly(alkyl methacrylate)s. As described above, now, we have the detailed and explicit information on the ordered structures in PF−Hm−Fn−Y series, such as the ordering and softening of the main backbone chains and the side chains which are temperature-dependent. In general, the dielectric spectroscopic measurements can detect the molecular motion of polymers through the dipole moment as the indicator. In PX−Hm−Fn−Y, the partial dipole moments are considered to exist in α-CX of the main backbone chains, and −COO−, CH_2-CF_2-, and ω-CF_2H of the side chains, whose polar moieties may be key points to determining the structure and properties. Therefore, it is worthy to investigate the segmental molecular motion of PX−Hm−Fn−Y by dielectric relaxation studies.

In the present work, we systematically investigate dielectric relaxation in homologous series of PX−Hm−Fn−Y to explore the segmental molecular motion. The mechanism of the segmental molecular motion is disclosed, based on the chemical structure and the orderings of main backbone and fluoroalkyl side chains. In particular, the local molecular motion of the fluoroalkyl side chains (γ relaxation) is well explained by compass motion model newly proposed in this paper.

Experimental Section

The PX−Hm−Fn−Y polymers used here are listed in Table 1 with their physical properties. Both PF−H1−Fn−Y and PX−H2−F8−F are those synthesized previously,[11,12] and this synthetic procedure was essentially used for the other PF−Hm−Fn−Y polymers; fluoroalkyl α-fluoroacrylate monomers were prepared by a dehydrogen fluoride reaction of α-fluoroacryloxy fluoride with the corresponding fluoroalkyl alcohol. The PF−Hm−Fn−Y polymers were obtained by a radical polymerization of the corresponding α-fluoroacrylate monomer in 1,3-bis(trifluoromethyl)benzene, using AIBN as an initiator and isooctyl mercaptoacetate as a molecular weight regulator in a sealed Pyrex tube. The polymers obtained were heated at 453−533 K under reduced pressure for 24 h to remove unreacted monomer and other volatiles. Elementary analyses were carried out with a Yanaco CHN CORDER MT-5 elemental analyzer with a fluoride-selective electrode (ORION RESEARCH microprocessor ion analyzer 901) to confirm the purity. Weight-average molecular weights (M_w) were determined by a gel permeation chromatography, using tetrahydrofuran (THF) as eluent and polystyrene as a standard. Intrinsic viscosities $[\eta]$ were measured in ethyl acetate or 1,3-bis(trifluoromethyl)benzene (see Table 1) at 308 K by use of an Ubbelohde viscometer. The values of M_w and $[\eta]$ listed Table 1 show that the polymers had high enough molecular weight to be regarded as a polymeric system. The stereoregularity (triad tacticity) was determined from NMR spectroscopy by almost the same procedure as described before;[11,12] ^{19}F NMR spectra were recorded on a 282 MHz ^{19}F NMR spectrometer (Bruker, AC-300P), using acetone as a solvent and monofluorotrichloromethane ($CFCl_3$) as an internal standard for PF−Hm−Fn−Y and PC−H2−F8−F, and those for the other insoluble polymers were measured in a molten state above the melting point (T_m) by use of a 93.7 MHz ^{19}F NMR spectrometer (JEOL, FX-100), using trifluoroacetic acid (TFA) as an internal standard. The peak splitting attributing to the α-F (or Cl)

region of the spectra were observed around −160 to −170 ppm with $CFCl_3$ reference and 80 to 90 ppm with TFA. Triad tacticities were estimated from the intensity ratios of three peaks according to Majumder and Harwood.[16] ^{1}H NMR for PM−H2−F8−F and ^{13}C NMR for PA−H2−F8−F spectra were measured by use of a 300 MHz ^{1}H NMR spectrometer (Bruker, AC-300P) and a 75 MHz ^{13}C NMR spectrometer (Bruker, AC-300P), respectively. Triad tacticities were obtained from the three split peaks of α-CH_3 for PM−H2−F8−F and the peaks of C=O for PA−H2−F8−F.

Thermal data were measured at a heating rate of 10 K min^{-1}, using a differential scanning calorimeter (DSC) (Perkin-Elmer, DSC-7). Glass transition temperature (T_g), melting point (T_m), and the enthalpy change (ΔH_m) were determined from the first DSC heating curves.

Dielectric measurements were carried out with a multifrequency LCR meter (YHP, type 4274A) at a heating rate of about 2 K min^{-1} in the temperature range 80−530 K and at 11 frequencies between 100 Hz and 100 kHz. The three-terminal-electrode system constructed previously[17] was used for the dielectric measurements: The electrode consists of main and unguarded electrodes which are disks of 37 and 50 mm diameter, respectively. The main electrode is guarded with the guard disk electrode of 50 mm o.d. and 39 mm i.d. which is set on one flat insulating plate (steatite) concentrically with the main electrode. As a result, the gap between the main and the guard electrodes is 1 mm. The sheet sample was sandwiched between the main (guarded) and unguarded electrodes and is lightly loaded by springs. The surface of sheet was aluminum-deposited to ensure the electric contact between the sheet and the electrode. This electrode system was mounted in the shield box which is filled with N_2 after sealing under reduced pressure. The measurements at high temperatures to over T_m were done by use of another electrode system described previously,[18] where the main (guarded) electrode is spaced from the unguarded electrode with a glass spacer 0.2 mm thick. Concretely, the electrode cell consists of main and unguarded electrodes which the polymer sheet was sandwiched between. This cell was once heated above T_m of the polymer under a load by the springs and cooled to room temperature at a rate of about 15 K min^{-1}, and then the dielectric measurements were started.

Dielectric Relaxation Behavior

PF−H1−Fn−Y. Figure 2 shows temperature dependences of dielectric constant (ϵ') and the loss (ϵ'') for PF−H1−F2−F at different frequencies. There are observed two relaxations, α near 424 K and γ near 123 K at 1 kHz, being essentially consistent with our previous dielectric results for a few PF−H1−Fn−F polymers.[13] Referring to the assignments for poly(alkyl methacrylate)s reported by several researchers,[19,20] the α and γ relaxations are attributable to a reorientational molecular motion of long segments above T_g and a local molecular motion of the fluoroalkyl side chains below T_g, respectively. An unusual peak of ϵ' is seen near 506 K, increasing in height at lower frequencies. The increase in ϵ'' at the highest temperatures may be due to ionic conduction,[18] while the peak in both ϵ' and ϵ'' may be caused by the melting of the crystallites, because the temperature exhibiting the peak corresponds with T_m, independent of frequency. Figure 3a shows temperature dependences of dielectric loss (ϵ'') at 1 kHz for PF−H1−Fn−F homologous series in the temperature range below 350 K, and Figure 3b gives those of log ϵ'' at 1 kHz and the loss tangent (tan δ) at 100 kHz in the higher temperature range above 300 K. In Figure 3a, the γ relaxation is seen between 100 and 175 K for the $n = 2-11$ homologues and the β relaxation is recognized between 250 and 300 K for the $n = 7-9$ homologues. In the $n = 1$ homologue, the γ relaxation does not exist,

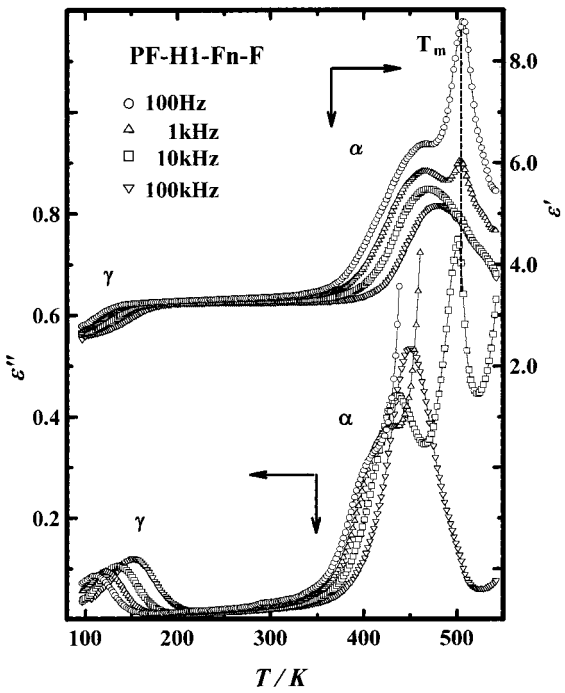

Figure 2. Temperature dependence of dielectric constant (ϵ') and the loss (ϵ'') for PF−H1−F2−F at different frequencies.

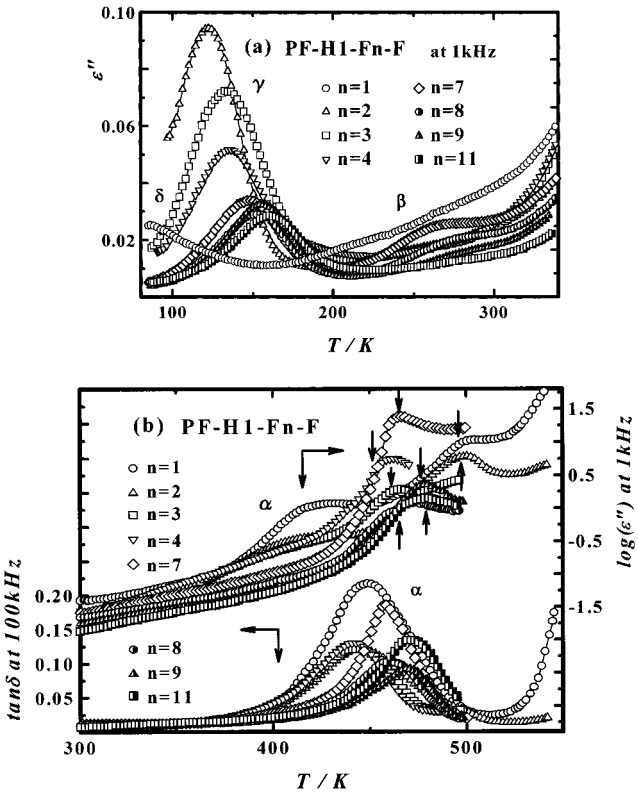

Figure 3. (a) Temperature dependences of dielectric loss (ϵ'') at 1 kHz in the lower temperature range below 350 K, and (b) temperature dependences of log ϵ'' at 1 kHz and the loss tangent (tan δ) at 100 kHz in the higher temperature range above 300 K for PF−H1−Fn−F homologues. Arrows show T_m.

and instead, the δ relaxation appears as a skirt in the lower temperature range below 100 K. On the basis of the assignments of poly(*n*-alkyl methacrylate)s again,[19−21] we can assign the β and δ relaxations to an internal rotation of carbonyl group and an internal rotation of ethyl group (−CF_2−CF_3), respectively.[20] As the length

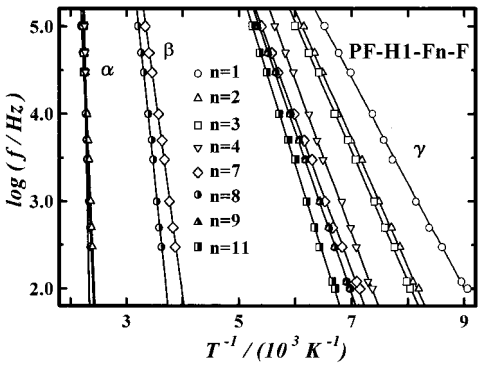

Figure 4. Arrhenius plots of logarithms of frequency (log *f*) versus $1/T_{max}$ for PF−H1−Fn−F, where T_{max} is the temperature exhibiting the relaxation peak at a frequency on ϵ''−temperature plots.

of the fluoroalkyl side chains (N_c) increases, the γ relaxation shifts to higher temperatures and gradually decreases in intensity. The β relaxation is not seen when $N_c \leq 4$ but is largest when $N_c = 7$, then decreasing with increasing N_c. In log ϵ''−temperature plots of Figure 3b, the α relaxation is observed for the $n = 1$ and 2 homologues but veiled for the $n = 3-11$ by the rapid increase of ϵ'' at higher temperatures which may be due to an ionic conduction. The peak of log ϵ'' at high temperatures may be caused by the melting of crystallites, because each peak temperature corresponds to each melting point (T_m, see arrow in Figure 3b). On tan δ−temperature curves, on the other hand, the α relaxation is clearly seen for all the homologues. As the length of side chains (N_c) increases, the α relaxation slightly moves to lower temperatures when $N_c \leq 4$ but shifts to higher temperatures when $N_c > 4$.

Figure 4 shows Arrhenius plots of logarithms of frequency (log *f*) versus $1/T_{max}$ for all PF−H1−Fn−F used here, where T_{max} is the temperature exhibiting the relaxation peak at a frequency on ϵ''−temperature plots. In the γ and β relaxations, the plots are on a straight line, indicating an Arrhenius type, while those for the α relaxation are curved, showing a WLF type. The activation enthalpies (ΔH) for the γ and β relaxations and the WLF parameters for the α relaxation are listed in Table 2. The value of ΔH is estimated as 23−40 kJ mol^{-1} for the γ relaxation and 90−118 kJ mol^{-1} for the β relaxation which support the assignments for the β and γ relaxations described above. The value of ΔH for γ relaxation gradually increases with increasing N_c. In the α relaxation, the free volume at T_g is 0.021−0.024, suggesting the α relaxation obeys the WLF theory.

Figure 5 shows temperature dependences of dielectric loss (ϵ'') for PF−H1−Fn−H series having CF_2−H at the terminal of the side chains. PF−H1−Fn−H as well as PF−H1−Fn−F shows α and γ relaxations; at 1 kHz, the α relaxation is seen in the $n = 2$ homologue but, in the $n = 4-8$ homologues, was veiled by the increase of ϵ'' due to an ionic conduction at higher temperatures above 300 K (not shown in Figure 5). The γ relaxation locates around 140 K, being independent of N_c in contrast with that for PF−H1−Fn−F (Figure 3a), and is much larger in intensity, compared with that for PF−H1−Fn−F. The β relaxation is not seen for all PF−H1−Fn−H polymers. The values of ΔH for the γ relaxation are estimated to be 33−59 kJ mol^{-1}, as shown in Table 2, being larger than those for the corresponding PF−H1−Fn−F, and increase with increasing N_c, and this increment is considerably larger, compared with that in PF−H1−Fn−F. These interesting results are discussed in detail later.

PX−H2−Fn−F. Figure 6 shows temperature dependences of dielectric loss (ϵ'') at 1 and 100 kHz for the PF−H2−Fn−F series. The α, β, and γ relaxations are all observed. As N_c increases, both α and γ relaxations shift to higher temperatures and decrease in intensity. It is noted that the β relaxation is clearly seen between 250 and 300 K, and its intensity is dependent on N_c, showing a maximum value when $n = 6$ ($N_c = 8$). The values of ΔH are estimated to be 28−37 kJ mol^{-1} for the γ relaxation and 85−136 kJ mol^{-1} for the β relaxation (Table 2).

Temperature dependences of ϵ'' at 100 kHz are shown in Figure 7 for PX−H2−F8−F. The dielectric relaxation behavior changes with the X substituent in a complicated manner. In PF−H2−F8−F, the α, β, and γ relaxations are observed as described above. The γ relaxation is observed near 190 K at 100 kHz, being unchanged with the X subsutituent. The β relaxation appears for the X = F and methyl (M) subsutituents, although the intensity in the latter substituent is very weak. The change in the α relaxation by the X subsutituent is interesting. The α relaxation appears near 440 K at 100 kHz for PF−H2−F8−F and shifts to lower temperatures in the order of F, Cl, M, and H of X. In PH−H2−F8−F, the α relaxation is seen only as a skirt above T_m and disappears below T_m, causing an abrupt change in ϵ'' at T_m. This abrupt change at T_m appears to faintly exist in PM−H2−F8−F ($T_m = 361$ K) and PC−H2−F8−F ($T_m = 404$ K) but is not visualized for PF−H2−F8−F. Therefore, the α relaxation, due to a reorientational molecular motion of long segments, is somewhat restricted by the ordering of the fluoroalkyl side chains and the releasing from the ordering at T_m make the appearance of the α relaxation. Actually, the degree of the abrupt change seems to be correlated with the melting enthalpy change (ΔH_m) in Table 1, and this result seems to be reasonable, because ΔH_m replies to the degree of crystallinity.

Other α-Fluoroacrylate Polymers. In Figure 8, the values of ϵ'' at 1 kHz are plotted against temperature for PF−H2−H, PF−H3−H, and PF−HFIP with PF−H1−F1−F and PF−H1−F2−F. As described already, PF−H1−F1−F has the α and δ relaxations, while PF−H1−F2−F shows the α and γ relaxations. PF−H2−H and PF−HFIP show the α relaxation but not the γ relaxation, while PF−H3−H shows the α and γ relaxations. These results are essentially consistent with those for PF−H1−F1−F and PF−H1−F2−F. The γ relaxation is caused by the local molecular motion of alkyl side chains and is inactive for the ethyl ester, and here the δ relaxation takes place in the lower temperature range instead of the γ relaxation. The α relaxation appears around 420−430 K at 1 kHz in PF−H1−F1−F and PF−H1−F2−F but locates at the lower temperature range in PF−H2−H and at much lower temperatures in PF−H3−H, which may be explained by a plasticization effect of the flexible alkyl group, as have been reported for poly(alkyl methacrylate)s.[19,20] In PF−HFIP, the α relaxation lays at higher temperatures than that in PF−H3−H, which may be caused by a steric hindrance of the branched alkyl ester.

Summary of Experimental Dielectric Relaxations. Consequently, the PF−Hm−Fn−Y polymers show α, β, and γ relaxations from the higher temperature side. The α, β, and γ relaxations are attributed

Table 2. Relaxation Parameters

	γ relaxation		β relaxation		α relaxation					
sample	T_{max} (K) at 1 kHz	$\Delta H(\gamma)$ (kJ mol^{-1})	T_{max} (K) at 1 kHz	$\Delta H(\beta)$ (kJ mol^{-1})	T_{max} (K) at 1 kHz	T_{max} (tan δ) (K) at 100 kHz	T_0 (K)	C_{1g}	C_{2g}	f_g
PF−H1−F1−F					429	449	302	41	81	0.024
PF−H1−F2−F	123	23			424	445	314	48	56	0.021
PF−H1−F3−F	134	28				444				
PF−H1−F4−F	135	28				442				
PF−H1−F7−F	147	34	266	90		457				
PF−H1−F8−F	153	34	283	118		460				
PF−H1−F9−F	156	36				469				
PF−H1−F11−F	161	40				471				
PF−H1−F2−H	149	33			407	432	270	36	89	0.027
PF−H1−F4−H	151	42				423				
PF−H1−F6−H	139	52				431				
PF−H1−F8−H	143	59				439				
PF−H2−F4−F	136	28	269	85	385	409				
PF−H2−F6−F	148	31	272	124	398	418				
PF−H2−F8−F	158	37	285	136	408	434	265	54	68	0.019
PF−H2−F10−F	163	37				442				
PH−H2−F8−F	163	39								
PM−H2−F8−F	158	37	290	122[a]		377				
PC−H2−F8−F	161	37				424				
PF−HFIP					408	432	347	24	28	0.041
PF−H2−H					393	412	273	30	94	0.033
PF−H3−H	120	23			371	390	317	29	18	0.034

[a] Quenched sample.

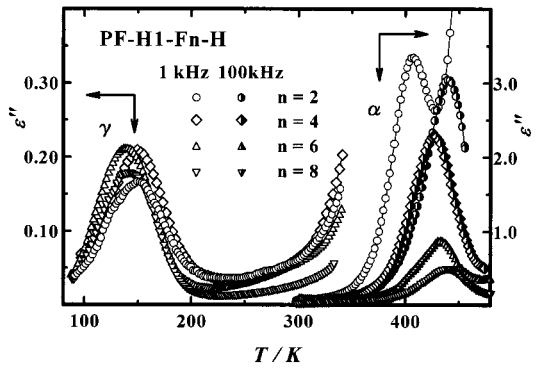

Figure 5. Temperature dependences of dielectric loss (ϵ'') for PF−H1−Fn−H series.

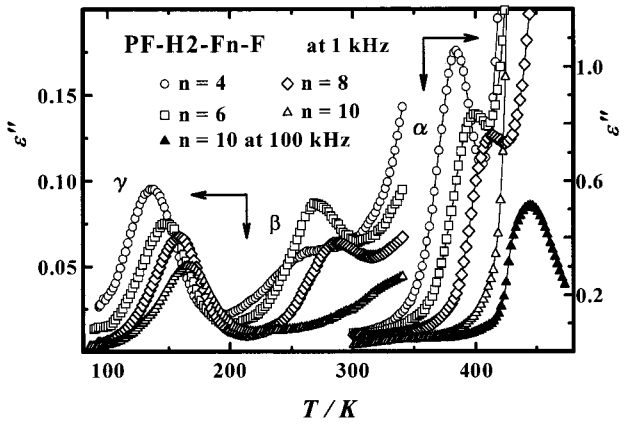

Figure 6. Temperature dependences of dielectric loss (ϵ'') at 1 kHz for PF−H2−Fn−F series. The data are shown at 1 and 100 kHz for the $n = 10$.

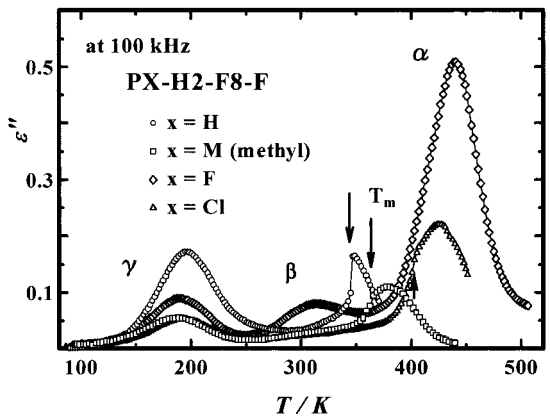

Figure 7. Temperature dependences of dielectric loss (ϵ'') at 100 kHz for PX−H2−F8−F.

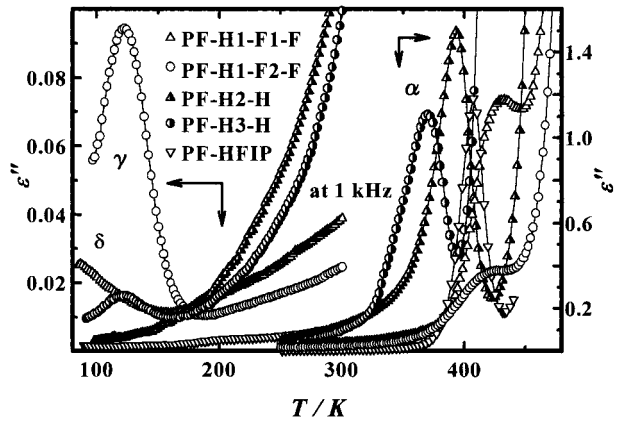

Figure 8. Temperature dependences of dielectric loss (ϵ'') at 1 kHz for PF−H2−H, PF−H3−H, and PF−HFIP with PF−H1−F1−F and PF−H1−F2−F.

respectively to a reorientational molecular motion of long segments above T_g, an internal rotational motion of carbonyl group in the amorphous region, and a local molecular motion of fluoroalkyl side chains below T_g. In poly(*n*-alkyl methacrylate)s and poly(*n*-alkyl acrylate)s, as is well-known,[19,21] the α relaxation moves to lower temperatures and the γ relaxation moves inversely to higher temperatures, as the alkyl length (N_c) increases. In PF−Hm−Fn−F ($m = 1$ or 2), both α and γ relaxations move to higher temperatures as N_c increases. The shift of α relaxation to higher temperatures may be caused by the rigidity of the side chain; the

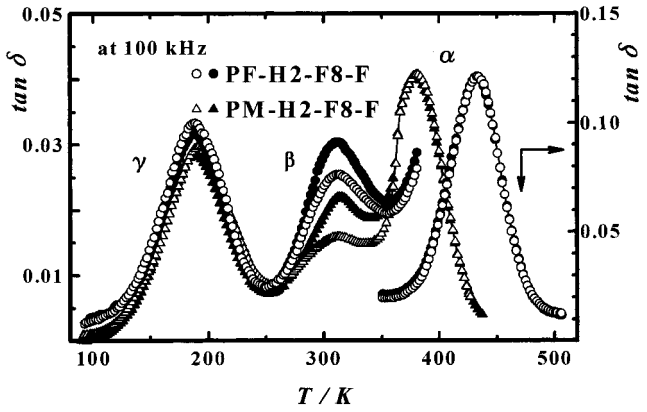

Figure 9. Variation of the relaxations with thermal history in PF−H2−F8−F and PM−H2−F8−F. Open symbols: samples cooled to room temperature at a rate of about 1.5 K min^{-1} from the molten states. Closed symbols: samples quenched into liquid nitrogen from the molten states.

flexible *n*-alkyl side chains move the α relaxation to lower temperatures due to the plasticization effect, while the fluoroalkyl side chain is rigid, moving the α relaxation to higher temperatures. On the other hand, the γ relaxation is modified with N_c and the chemical structure such as the terminal moiety of the side chain ($-CF_2Y$) and α substituent (X): In PF−H1−Fn−F and PM−H1−Fn−F, the relaxation temperature (T_{max}) is higher with the increase of N_c but is unchanged in PF−H1−Fn−H. It is noticed that the value of $\Delta H(\gamma)$ increases rather proportionally to the N_c value, and the increment is larger in the PF−H1−Fn−H series than the PF−Hm−Fn−F series. These results remind us of the existence of an intermolecular hydrogen bonding produced by the terminal $-CF_2H$ group. From these viewpoints, we newly proposed "compass motion model" for the γ relaxation in the next section.

Variation of the relaxations with thermal history is shown for PF−H2−F8−F and PM−H2−F8−F in Figure 9. The α and γ relaxations are scarcely changed by the thermal treatment, but the β relaxation clearly increases in intensity by quenching for both polymers. Therefore, we concluded that the β relaxation is related to an internal rotational motion of carbonyl group in the amorphous region. As described already, the α relaxation is assigned to be a reorientational motion of long segments above T_g, obeying the WLF type. We, therefore, believe that the α relaxation takes place above T_m, as is easily understood in PH−H2−F8−F of Figure 7. Above T_m, the polymer is in the liquid state and amorphous, resulting in making the α relaxation independent of the thermal treatment: In PF−Hm−Fn−Y and PC−H2−F8−Y, the α relaxation, however, appears even at temperatures below T_m. Inferring from these results, the molecular motion of long segments would begin to occur even in the crystalline region below T_m. As already described in the Introduction, our previous X-ray diffraction results indicate that both main backbone and fluoroalkyl side chains are ordered to form the crystallites at room temperature. As temperature increases, the ordering of main backbone chains begins to decrease near T_g below T_m, while an ordering of the side chains still remains above T_m. However, the packings would be so loose that the main backbone chains could respond to the applied ac electric field, resulting in the appearance of the α relaxation below T_m.

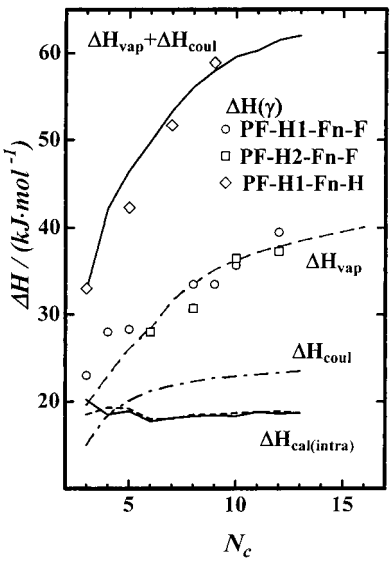

Figure 10. Plots of activation enthalpy [$\Delta H(\gamma)$] for the γ relaxation versus N_c in PF−Hm−Fn−Y polymers. Curves for the potential energy ($\Delta H_{cal(intra)}$) calculated by the MM2 method for model compounds: (—) $(CH_3)_2CF-COOCH_2(CF_2)_n-F$ (MF−H1−Fn−F) for PF−H1−Fn−F, (- - -) $(CH_3)_2CF-COOCH_2-(CF_2)_n-H$ (MF−H1−Fn−H) for PF−H1−Fn−H, (— — —) the vaporization enthalpy (ΔH_{vap}) for C_nF_{2n+2}, (— - —) the Coulomb force energy (ΔH_{coul}) calculated from eq 5, and (—) [ΔH_{vap}+ΔH_{coul}] versus N_c curves for MF−H1−Fn−H.

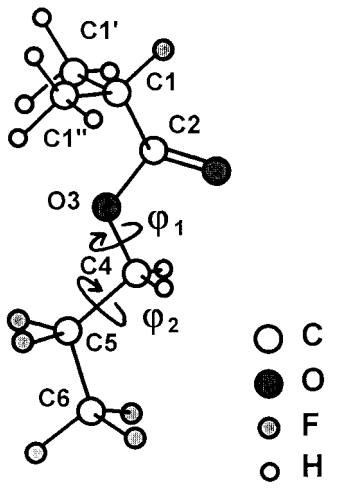

Figure 11. Most stable structure of MF−H1−F2−F obtained from the MM2 method and torsional angles, φ_1 and φ_2.

Compass Motion Model for the γ Relaxation

By numerous dielectric and dynamic mechanical relaxation studies for poly(*n*-alkyl methacrylate)s,[19−22] it has been established that the γ relaxation arises mostly from the internal rotation of alkyl groups and exists in poly(*n*-alkyl methacrylate)s with an alkyl group longer than the ethyl group. The potential energy calculation of the internal rotation in the alkyl side group has been made for poly(*n*-butyl methacrylate). In particular, Shimizu, Yano, and Wada[21] calculated the potential energy of the internal rotation of butyl side group and pointed out that the rotation around C4−C5 axis (φ_2, see Figure 11) predominantly contributes to the γ relaxation. Their work is considered to clearly show that the γ relaxation comes from the internal rotation of the alkyl side chain.

As described before, the γ relaxation also exists in the present PX−Hm−Fn−Y polymers, corresponding to that

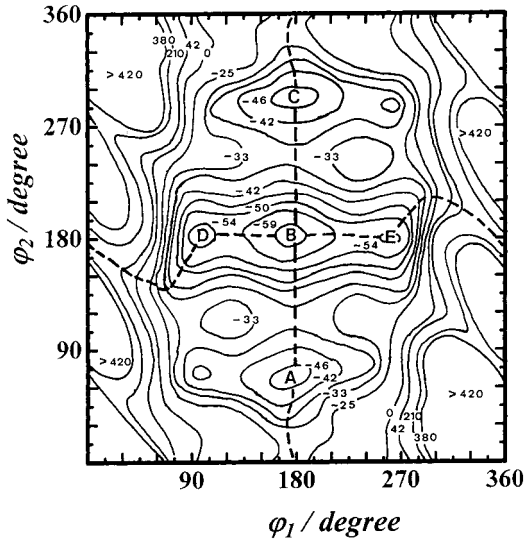

Figure 12. Potential energy (U) counter map as functions of φ_1 and φ_2 for MF−H1−F2−F, where φ_1 is an angle of C−O to CH_2-CF_2 bond in $-O-CH_2-CF_2-CF_3$ when the CH_2-CF_2 bond rotates to the right around the C−O bond, and φ_2 is an angle of CH_2-CF_2 bond to CF_2-CF_3 bond rotating to the right around the CH_2-CF_2 bond. The unit of values in the figure is kJ mol^{-1}.

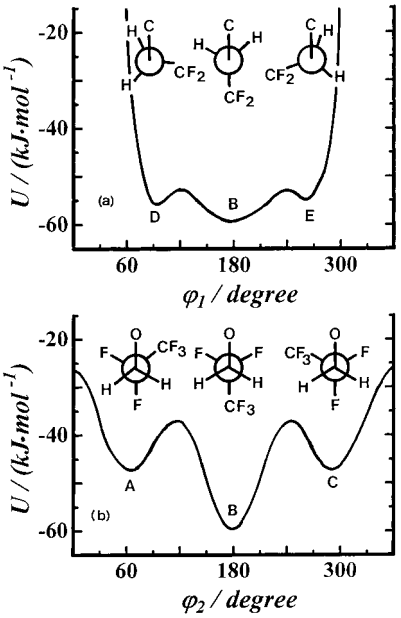

Figure 13. Potential curves for φ_1 when φ_2 is 180° (U versus φ_1 when $\varphi_2 = 180°$) (a) and U versus φ_2 curve when $\varphi_1 = 180°$ (b).

in poly(*n*-alkyl methacrylate)s, and significantly changes by the chemical structure, the length and terminal group of side chain, and the X subsutituent.

Figure 10 shows plots of activation enthalpy change, $\Delta H(\gamma)$, for the γ relaxation versus N_c in PF−Hm−Fn−Y polymers. Remarkably, the value of $\Delta H(\gamma)$ increases with increasing N_c, and the increment of $\Delta H(\gamma)$ with N_c is larger in PF−Hm−Fn−H than PF−Hm−Fn−F. We calculated the potential energy for internal rotation of the fluoroalkyl side chains, where we used two model compounds, $(CH_3)_2CF-COOCH_2(CF_2)_n-F$ (MF−H1−Fn−F) for PF−H1−Fn−F and $(CH_3)_2CF-COOCH_2-(CF_2)_n-H$ (MF−H1−Fn−H) for PF−H1−Fn−H, to get a potential energy map of the internal motion in the side chain with the different fluoroalkyl length (N_c), responsible for the γ relaxation. Here, we assumed that the α-F in the main backbone chains is in a cis conformation to the C═O and the other C−C bonds are in a planar-zigzag structure conformation, because in PF−H1−Fn−F/H polymers, the α-F bond was found to be in a cis conformation to the C═O bond in the crystallites from our IR and X-ray diffraction studies.[11,23] Then, we calculated the most stable molecular structure for the two model compounds, MF−H1−Fn−F and MF−H1−Fn−H, by use of Parametric Method 3 (PM3), and the structure obtained is shown for MF−H1−F2−F in Figure 11. On the basis of this molecular structure, we calculated the change of potential energy with the torsion angles of φ_1 and φ_2 by use of the Molecular Mechanics 2 (MM2) method, where φ_1 is an angle of the C−O to CH_2-CF_2 bond in $-O-CH_2-CF_2-CF_3$ when the CH_2-CF_2 bond rotates to the right around the C−O bond, and φ_2 is an angle of the CH_2-CF_2 bond to CF_2-CF_3 bond rotating to the right around the CH_2-CF_2 bond. The counter map of potential energy (U) obtained is drawn in Figure 12 as functions of φ_1 and φ_2 for MF−H1−F2−F. We also calculated the potential energies (U) for MF−H1−Fn−F and further MF−H1−Fn−H with different side chain length (n) which were almost equal to that for MF−H1−F2−F. The potential energy counter map of Figure 12 shows five minima at A−E points. Therefore, it is possible that the structural changes advance through two routes, D ⇔ B ⇔ E ⇔ D and A ⇔ B ⇔ C ⇔ A. Clearly, D ⇔ B ⇔ E ⇔ D transitions occur mostly by the change of φ_1 when φ_2 is about 180°, while the A ⇔ B ⇔ C ⇔ A goes mostly by the change of φ_2 when φ_1 is about 180°. Figure 13 shows the potential curve for φ_1 when φ_2 is 180° (U versus φ_1 when $\varphi_2 = 180°$) and U versus φ_2 curve when $\varphi_1 = 180°$. Both curves give three stable conformational structures which locate at the minimum points of U. In D ⇔ B ⇔ E ⇔ D, the activated energies of D ⇔ B ⇔ E and E ⇔ D transitions have about 2 and 140 kJ mol^{-1}, respectively, which much deviate from that of γ relaxation (23−40 kJ mol^{-1}). While, in A ⇔ B ⇔ C ⇔ A, the activated energies of A ⇔ B ⇔ C and C ⇔ A transitions have about 10 and 20 kJ mol^{-1}, respectively. Therefore, it is considered that the A ⇔ B ⇔ C ⇔ A route may be responsible for the γ relaxation.

According to the two-state transition theory by Hayakawa, Tanabe, and Wada,[24] the dielectric increment ($\Delta\epsilon$) is expressed as follows

$$\Delta\epsilon = [4\pi N(\Delta\mu)^2/3RT][(\epsilon_\infty + 2)/3]^2[3\epsilon_0/(2\epsilon_0 + \epsilon_\infty)]K/(1+K)^2 \quad (1)$$

where

$$K = \exp(-\Delta U/RT) \quad (2)$$

where N, $\Delta\mu$, R, ϵ_0, ϵ_∞, K, and ΔU are the molar number of motional units per unit volume, the change of dipole moment in vacuo induced by the transition, gas constant, the low-frequency limiting dielectric constant, high-frequency limiting one, the equilibrium constant of the transition, and the difference in a potential energy between two states, respectively. In eq 1, the value of $\Delta\epsilon$ is proportional to $K/(1+K)^2$, and so when $K = 1$, $K/(1+K)^2$ takes a maximum value of $^1/_4$. Therefore, a transition path with a maximum K value may be responsible for the γ relaxation. In Figure 12, φ_1, φ_2, and U are 175°, 65°, and −47.2 kJ mol^{-1} at A, 180°,

Table 3. Energetic Parameters for Molecular Motion of Fluoroalkyl Chains

N_c	$\Delta H(\gamma)$ (kJ mol^{-1})	MM2 $\Delta H_{cal(intra)}$ (kJ mol^{-1})	ΔH_{vap} (kJ mol^{-1})	$\Delta H_{coh} = \Delta H_{vap} - \Delta H_{cal(intra)}$ (kJ mol^{-1})	H---F ΔH_{coul} (kJ mol^{-1})
	PF−H1−Fn−F	MF−H1−Fn−F	C_nF_{2n+2}[d]		
3	23.0	20.2	19.6	−0.6	
4	28.0	18.5	22.9	4.4	
5	28.3	18.9	26.1	7.2	
6		17.7	28.3	10.6	
7		18.1	31.6	13.5	
8	33.5	18.3	33.6[b]	15.3	
9	33.5	18.4	35.2[a]	16.8	
10	35.7	18.3	36.3[b]	18.0	
11		18.8	37.2[b]	18.4	
12	39.5	18.6	37.9[b]	19.3	
13		18.7	38.5[b]	19.8	
16			40.1[a]		
	PF−H1−Fn−H	MF−H1−Fn−H	$C_nF_{2n+1}H$[d]		
3	33.0	18.5			15.0
4		19.3			18.5
5	42.3	19.2			20.1
6		18.0			21.2
7	51.7	18.0	32.5[a]	14.5	21.8
8		18.5			22.3
9	58.9	18.5			22.7
10		18.7			22.9
11		18.8			23.1
12		18.9			23.3
13		18.7			23.5
	PF−H2−Fn−F	MF−H2−Fn−F			
3		20.1			
4		19.1			
5		20.5			
6	28.0	18.8			
7		20.2			
8	30.7	20.4			
9		20.1			
10	36.5	20.0			
11		20.2			
12	37.3	20.1			
13		20.3			
	PF−H3−H	MF−Hn−H	C_nH_{2n+2}[e]		
3	23.1	13.9	19.0		
	PM−Hn−H	MM−Hn−H			
3	16.8[c]	14.8	18.8		
4	23.0[c]	15.1	22.4		
8	20.9[c]	15.1	34.9		
12	32.6[c]	15.2	43.0[a]		
16	37.8[c]	15.2	48.6[a]		

[a] Calculated from Trouton's rule. [b] The value extrapolated to T_b. [c] Data from refs 22 and 27−29. [d] Data from ref 25. [e] Data from ref 26.

180°, and −59.3 kJ mol^{-1} at B, and 180°, 290°, and −47.0 kJ mol^{-1} at C, which correspond to gauche, trans, and antigauche conformations, respectively. The ΔU values for the A ⇔ B, B ⇔ C, and C ⇔ A are estimated as 12.1, 11.9, and 0.2 kJ mol^{-1}, respectively and so it was concluded that the C ⇔ A transition and the gauche ⇔ antigauche conformational change are associated with the γ relaxation. The activation enthalpy ($\Delta H_{cal(intra)}$) for the C ⇔ A route was calculated for the MF−H1−Fn−F and MF−H1−Fn−H homologues, and their data are listed in Table 3. The value of $\Delta H_{cal(intra)}$ shows almost a constant value of 19 kJ mol^{-1}, almost independent of n for both homologues. These $\Delta H_{cal(intra)}$ values, of course, are for an isolated compound at 0 K. The enthalpy changes (ΔH_{vap}) of vaporization at boiling point (T_b) under 1 atm are listed for C_nF_{2n+2} homologues[25] in Table 3, where those of C_9F_{20} and $C_{16}F_{34}$ were estimated from T_b by use of Trouton's law ($\Delta H_{vap} = 87.9T_b$). The change of $\Delta H_{cal(intra)}$ and ΔH_{vap} with N_c is given in Figure 10. The $\Delta H_{cal(intra)}$ shows a constant value of about 19 kJ mol^{-1}, almost independent of N_c, but appears to slightly fluctuate around 6 of N_c. This fluctuation might be connected with the change of the ordered structure by N_c; when $N_c < 7$, the ordering of the main backbone chains but that of the fluoroalkyl side chains when $N_c \geq 7$ predominate in the formation of crystallites as described in the Introduction, and the degree of crystallinity shows a minimum around $N_c = 6$. Rather surprisingly, the activation enthalpy for γ relaxation obtained from dielectric measurements [$\Delta H(\gamma)$] falls well on the $\Delta H_{vap}-N_c$ curve. At $N_c = 3$, the value of $\Delta H(\gamma)$ is about 23 kJ mol^{-1}, being consistent with $\Delta H_{cal(intra)}$, but as N_c increases more, it deviates from $\Delta H_{cal(intra)}$ and moves on the $\Delta H_{vap}-N_c$ curve. As temperature increases to T_b, ΔH_{vap} commonly decreases, and ΔH_{vap} at T_b is interpreted as an energy that is necessary to overcome the intramolecular and intermolecular interaction in the liquid state and to transform into the gaseous state. Therefore, $\Delta H(\gamma)$ is expressed as

$$\Delta H(\gamma) = \Delta H_{vap} = \Delta H_{intra} + \Delta H_{inter} \quad (3)$$

where ΔH_{inter} is an intermolecular interaction (cohesion) energy change. As described above, the γ relaxation is attributed to the intramolecular rotation about the

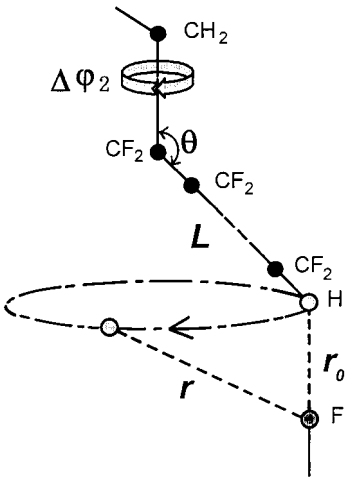

Figure 14. "Compass motion model" for the γ relaxation in PF−H1−Fn−H.

$-CH_2-CF_2-$ axis in the side chain, but this rotational motion may result from overcoming the intermolecular interaction between the side chains.

In the PF−H1−Fn−H homologue having the terminal group, $-CF_2H$, $\Delta H(\gamma)$ is larger than that for the PF−H1−Fn−F homologue having the terminal group, $-CF_3$, and rapidly increases as N_c increases. Therefore, the value of $\Delta H(\gamma)$ for PF−H1−Fn−H is not explained simply by the ΔH_{vap} value for C_nF_{2n+2}. Unfortunately, we have no data for ΔH_{vap} of $C_nF_{2n+1}H$ but have only T_b (369.2 K) of $C_7F_{15}H$, from which we got ΔH_{vap} of 32.5 kJ mol^{-1} by Trouton's law. This ΔH_{vap} estimate is almost equal to that C_7F_{16} (31.6 kJ mol^{-1}). Therefore, we think that the large $\Delta H(\gamma)$ values for PF−H1−Fn−H may be caused by the existence of hydrogen bonding at the terminal $-CF_2H$, such as H- - -F, and perhaps the intermolecular hydrogen bonding of terminal $-CF_2H$ with α-F. Here, we now propose a "compass motion model" for the γ relaxation as shown in Figure 14. In PF−H1−Fn−F, the γ relaxation results mainly from the intramolecular rotation about $-CH_2-CF_2-$ of the side chain. Therefore, the side chain moves on a circular orbit which is drawn at a constant angle of θ by a compass having the rodlike fluoroalkyl chain. However, we assume that in PF−H1−Fn−H the γ relaxation is perturbed with H- - -F intermolecular hydrogen bonding whose length is r_0. As illustrated in Figure 14, we assume that this hydrogen bonding is formed by Coulomb attraction (f),

$$f = -(q_H q_F/4\pi\epsilon_0)(1/r_0^2) \qquad (4)$$

where q_H, q_F, ϵ_0, and r_0 are charge of H, charge of F, dielectric constant in a vacuum, and an equilibrium distance of H- - -F, respectively. When the γ relaxation occurs and so the rodlike side chain rotates by $\Delta\varphi_2$, which is the shift angle of φ_2 between the antigauche and gauche conformations in the C ⇔ A transition, the distance of the H- - -F bond changes into r. As a result, the following energy (ΔH_{coul}) is necessary to make the rotation.

$$\Delta H_{coul} = (q_H q_F/4\pi\epsilon_0)(1/r_0 - 1/r) = (q_H q_F/4\pi\epsilon_0)(1/r_0)(1 - r_0/r) \qquad (5)$$

where $(q_H q_F/4\pi\epsilon_0)(1/r_0)$ is equal to the intermolecular hydrogen bonding energy of H- - -F, which has been reported to be about 25 kJ mol^{-1} for hydrogen fluoride.[30] Therefore, we obtained ΔH_{coul} for PF−H1−Fn−H from the eq 5, which is listed in Table 4 and is shown as a function of N_c in Figure 10. Consequently, the value of $\Delta H(\gamma)$ is expressed for the PF−H1−Fn−H series as follows:

$$\Delta H(\gamma) = \Delta H_{intra} + \Delta H_{inter} + \Delta H_{coul} = \Delta H_{vap} + \Delta H_{coul} \qquad (6)$$

From Figure 10, we can understand easily that the value of $\Delta H(\gamma)$ for PF−H1−Fn−H is well consistent with the theoretical value of $\Delta H_{vap} + \Delta H_{coul}$ (eq 6).

Consequently, it was concluded that the γ relaxation is caused by the gauche−antigauche rotational motion of the $O-CH_2-CF_2-CF_2-$ bond about the CH_2-CF_2 bond (change of φ_2 in Figure 11).

The potential energy for internal rotation of the alkyl side chains was also calculated for the models MF−H2−Fn−F, MF−H3−H, and MH−Hn−H by the same procedure described above, and the data are listed in Table 3 with the value of $\Delta H(\gamma)$. The value of $\Delta H(\gamma)$ and $\Delta H_{cal(intra)}$ in PF−H2−Fn−F coincides with those in PF−H1−Fn−F within 3 kJ mol^{-1} for $\Delta H(\gamma)$ and 1 kJ mol^{-1} for $\Delta H_{cal(intra)}$, respectively, and so the change of $\Delta H(\gamma)$ with N_c is well fitted to that in ΔH_{vap} of C_nF_{2n+2}. In MF−H3−H and MM−Hn−H having an n-alkyl side chain, $\Delta H_{cal(intra)}$ is smaller by about 4 kJ mol^{-1} than that in PF−H1−Fn−F. The ΔH_{vap} of C_nH_{2n+2} is much larger than that of C_nF_{2n+2}, when $n \geq 12$, and as a result, $\Delta H(\gamma)$ largely deviates from ΔH_{vap}. It is well-known that n-C_nH_{2n+2} changes in the structure and property from monomeric to polymeric nature around $n = 12$ with increasing n, and hence, the rapid increase of ΔH_{vap} for n-C_nH_{2n+2} with $n \geq 12$ would result from the polymeric nature, for example such as an entanglements of n-alkyl chains. Actually, in PM−Hn−H, the value of $\Delta H(\gamma)$ considerably fluctuates with N_c but appears to correspond roughly to that for PF−H1−Fn−F when $n \leq 8$, while much smaller than that of ΔH_{vap} when $n \geq 12$, although it is necessary to obtain more convincing experimental data of $\Delta H(\gamma)$ for PM−Hn−H.

Table 4. Calculation of ΔH_{coul} (kJ mol^{-1}) Based on Compass Motion Model[a]

model compd	L (Å)	θ (deg)	r (Å)	ΔH_{coul}
MF−H1−F2−H	2.219	113.00	3.863	14.97
MF−H1−F3−H	3.619	112.59	5.991	18.53
MF−H1−F4−H	4.898	112.78	7.974	20.14
MF−H1−F5−H	6.286	112.98	10.143	21.18
MF−H1−F6−H	7.590	112.78	12.220	21.83
MF−H1−F7−H	8.961	112.80	14.392	22.31
MF−H1−F8−H	10.277	112.65	16.500	22.65
MF−H1−F9−H	11.643	112.74	18.663	22.92
MF−H1−F10−H	12.964	112.59	20.789	23.14
MF−H1−F11−H	14.324	112.59	22.959	23.31
MF−H1−F12−H	15.652	112.57	25.082	23.46

[a] L, ϕ, and r are denoted in Figure 14.

Conclusion

The PX−Hm−Fn−Y polymers showed three dielectric relaxations, α above 400 K, β around 250 K, and γ below 150 K, which are attributable to a reorientational motion of long segments above T_g, a rotational motion of carbonyl groups in the amorphous region, and an internal motion of fluoroalkyl side chains, respectively. PF−H1−F1−F and PF−H2−H having ethyl side group, however, do not have γ relaxation and instead showed

δ relaxation below 100 K, which is assigned as an internal rotation of ethyl groups. This relaxation behavior faithfully reflected the chemical structures and the ordered structures of main backbone and fluoroalkyl side chains. We found that the activation enthalpies for the γ relaxation [$\Delta H(\gamma)$] increase proportional to N_c. In PF−H1−Fn−F, moreover, the values of $\Delta H(\gamma)$ were well consistent with the vaporization enthalpies of the corresponding C_nF_{2n+2} (ΔH_{vap}), while $\Delta H(\gamma)$ in PF−H1−Fn−H was considerably larger than the corresponding ΔH_{vap}. This characteristic behavior of the γ relaxation was well explained by the newly proposed compass motion model. The value of $\Delta H(\gamma)$ is the sum of intramolecular interaction energy (ΔH_{intra}) of the fluoroalkyl side chain and intermolecular interaction energy (ΔH_{inter}), and $\Delta H(\gamma)$ for the PF−H1−Fn−Y polymers coincide with ΔH_{vap}. Using the MM2 method, it was found that the rotational motion about the CH_2-CF_2 bond in $-O-CH_2-CF_2-CF_2-$ is predominantly responsible for the γ relaxation, and the rotational energy (ΔH_{intra}) was estimated as about 19 kJ mol^{-1}, regardless of N_c. Therefore, ΔH_{inter} can be expressed by $\Delta H(\gamma) - \Delta H_{intra}$ which increases with increasing N_c. Consequently, the γ relaxation results from the rotational motion about the $-CH_2-CF_2-$ bond of the side chain, and hence the side chain moves like a compass (compass motion model). On the other hand, in PF−H1−Fn−H, the compass motion would be perturbed by the hydrogen bonding of the terminal $-CF_2H$ with F, resulting in the increase of $\Delta H(\gamma)$. Actually, the $\Delta H(\gamma)$ data are well fitted to the ($\Delta H_{vap} + \Delta H_{coul}$) versus N_c curves, where ΔH_{coul} is the energy of hydrogen bonding. These results suggest that the γ relaxation would occur by overcoming the energy of intra- and intermolecular interaction. For PF−H1−Fn−H, the relaxation is described instead by the transition between the energy minima A and C in Figure 12. The activation energy for the transition is, of course, $\Delta H(\gamma)$. It is interesting that the $\Delta H(\gamma)$ is almost equal to ΔH_{vap} for PF−H1−Fn−F and $\Delta H_{vap} + \Delta H_{coul}$ for PF−H1−Fn−H.

In this work, we can conclude that the γ relaxation obeys the compass motion model for the present PF−H1−Fn−F and PF−H1−Fn−H polymers. The question is open whether the compass motion model holds in the γ relaxation in various side-chain-containing (comb-shaped) polymers or not, for example, poly(*n*-alkyl methacrylate)s having flexible alkyl side chains, side-chain liquid crystalline polymers bearing the rigid mesogenic side chains separated by the flexible spacer from main backbone chains, and so on.

References and Notes

(1) Plate, N. A.; Shibaev, V. P. *Comb-Shaped Polymers and Liquid Crystals*; Plenum Press: New York, 1987; Chapters 1, 2.

(2) Pittman, A. G.; Ludwig, B. A. *J. Polym. Sci., Part A-1* **1969**, *7*, 3053.

(3) Takezawa, Y.; Tanno, S.; Taketani, N.; Ohara, S.; Asano, H. *J. Appl. Polym. Sci.* **1991**, *42*, 3195.

(4) Budovskaya, L. D.; Ivanova, V. N.; Oskar, L. N.; Lukasov, S. V.; Baklagina, Y. G.; Sidorovich, A. V.; Nasledov, D. M. *Vyskomol. Sordin. Ser. A* **1990**, *32*, (3), 561.

(5) Katano, Y.; Tomono, H.; Nakajima, T. *Macromolecules* **1994**, *27*, 2342.

(6) Koizumi, S.; Ohmori, A.; Shimizu, T.; Iwami, M. *Jpn. J. Appl. Phys.* **1992**, *31* (10), 3408.

(7) Koizumi, S.; Ohmori, A.; Shimizu, T.; Iwami, M. *Jpn. J. Surf. Sie. Soc.* **1992**, *13* (7), 418.

(8) Okawara, A.; Maekawa, T.; Ishida, Y.; Matsuo, M. *Polym. Prepr., Jpn.* **1991**, *40*, 3098.

(9) Volkov, V. V.; Plate, N. A.; Takahara, A.; Kajiyama, T.; Amaya, N.; Murata, Y. *Polymer* **1992**, *33*, 1316.

(10) Shimizu, T.; Tanaka, Y.; Kutsumizu, S.; Yano, S. *Macromolecules* **1993**, *26*, 6694.

(11) Shimizu, T.; Tanaka, Y.; Kutsumizu, S.; Yano, S. *Macromolecules* **1996**, *29*, 156.

(12) Shimizu, T.; Tanaka, Y.; Kutsumizu, S.; Yano, S. *Macromol. Symp.* **1994**, *82*, 173.

(13) Koizumi, S.; Tadano, K.; Tanaka, Y.; Shimizu, T.; Kutsumizu, S.; Yano, S. *Macromolecules* **1992**, *25*, 6563.

(14) Banks, R. E. *Organofluorine Chemicals and their Industrial Applications*; Ellis Horwood: Chichester, 1979.

(15) Maruo, T.; Ishibashi, S.; Nakamura, K. *J. Polym. Sci., Part A-2: Polym. Chem.* **1994**, *23*, 3211.

(16) Majumder, R. N.; Harwood, H. J. *Polym. Bull.* **1981**, *4*, 391.

(17) Koizumi, N.; Yano, S. *Bull. Chem. Res. Kyoto Univ.* **1969**, *47*, 320.

(18) Yano, S.; Tadano, K.; Aoki, K.; Koizumi, N. *J. Polym. Sci., Polym. Phys. Ed.* **1974**, *12*, 1875.

(19) McCrum, N. G.; Read, B. E.; Williams, G. *Anelastic and Dielectric Effects in Polymeric Solids*; Wiley: New York, 1967; Chapter 8.

(20) Hedvig, P. *Dielectric Spectroscopy of Polymers*; Adams Helger: Bristol, 1977; Chapter 4.

(21) Shimizu, K.; Yano, O.; Wada, Y. *J. Polym. Sci., Polym. Phys. Ed.* **1973**, *11*, 1641.

(22) Shimizu, K.; Yano, O.; Wada, Y. *J. Polym. Sci., Polym. Phys. Ed.* **1975**, *13*, 1959.

(23) Shimizu, T.; Tanaka, Y.; Ohkawa, M.; Kutsumizu, S.; Yano, S. *Macromolecules* **1996**, *29*, 3540.

(24) Hayakawa, Y.; Tanabe, Y.; Wada, Y. *J. Macromol. Sci. (Phys.)* **1973**, *B8*, 445.

(25) Simons, J. H., Ed. *Fluorine Chemistry;* Academic Press: New York, 1964; Vol. V, pp 176−179.

(26) Lide, D. R., Ed. *CRC Handbook of Chemistry and Physics*, 76th ed.; CRC: Boca Raton, FL, 1995; p 6-114. Dean, J. A., Ed. *Lang's Handbook of Chemistry*, 11th ed.; McGraw-Hill: New York, 1973; p 9.

(27) Hoff, E. A. W.; Robinson, D. W.; Willbourn, A. H. *J. Polym. Sci.* **1955**, *18*, 161.

(28) Kawamura, Y.; Nagai, S.; Hirose, J. *J. Polym. Sci. A-2* **1969**, *7*, 1559.

(29) Borisova, T. I.; Burshtein, L. L.; Shevelev, V. A.; Shibayev, V. P.; Plate, N. A. *Vysokomol. Soedin. A-13* **1971**, *No. 10*, 2332.

(30) Pauling, L. *The Nature of the Chemical Bond*, 3rd ed.; Cornell University Press: Ithaca, NY, 1960; p 416 (Fredenhagen, K. *Z. Anorg. Chem.* **1934**, *218*, 161).

MA981048O